Materials Research, Vol. 5, No. 3, 391-397, 2002.

Theoretical - Experimental Analysis of Cellular and Primary Dendritic Spacings during Unidirectional Solidification of Sn-Pb Alloys

*Otávio F.L. da Rocha[a], Cláudio A. Siqueira[b] and Amauri Garcia[c]**

[a]*Doctoral Student and Research Assistant,*
Department of Materials Engineering, UNICAMP,CEFET-PA
[b]*Doctoral Student and Research Assistant,*
Department of Materials Engineering, UNICAMP
[c]*Professor/Department of Materials Engineering /UNICAMP*
13083-970 Campinas - SP, Brazil

Received: September 27, 2001; Revised: July 10, 2002

Structural parameters as grain size, dendritic and cellular spacings, segregated products, porosity and other phases are strongly influenced by the thermal behavior of the metal/mold system during solidification, imposing a close correlation between this and the resulting microstructure. Several unidirectional solidification studies with the objective of characterizing cellular and dendritic spacings have been developed in large scale involving solidification in steady-state heat flow. The main objective of this work is to determine the thermal solidification parameters during the cellular/dendritic transition as well as to compare theoretical models that predict cellular and primary dendritic spacings with experimental results for solidification situations in unsteady-state heat flow. Experiments were carried out in a water cooled unidirectional solidification apparatus and dilute alloys of the Sn-Pb system were used (Sn 1.5wt%Pb, Sn 2.5wt%Pb and Sn 5wt%Pb). The upper limit of the Hunt-Lu cellular growth model closely matched the experimental spacings. The lower limit calculated with the Hunt-Lu dendritic model best generated the experimental results. The cellular/dendritic transition was observed to occur for the Sn 2.5wt%Pb alloy over a range of analytical cooling rates from 0.28 K/s to 1.8 K/s.

Keywords: *unidirectional solidification, cellular/dendritic spacings, cellular/dendritic transition, cellular and dendritic growth models*

1. Introduction

The cellular and dendritic spacings are important microstructural parameters resulting from the solidification process, because it is known that these spacings have a significant influence on the properties of castings. They affect the microscopic segregation existing between the cellular or dendritic ramifications, having an influence on the mechanical behavior[1].

Several important theoretical[2-7] and experimental[8-13] studies have been developed with the object of selecting cellular and primary dendritic spacings. Among the theoretical models existing in the literature only that proposed for Hunt and Lu[4] assumes conditions of solidification in unsteady-state heat flow. Those proposed by Hunt, and Kurz and Fisher are based on steady-state. The theoretical models for determination of cellular and dendritic spacings proposed by these authors are shown in Eq. 1 to 6, respectively :

$$\lambda_1 = 2.83\left[\Gamma m_L C_0 (1-k_0) D\right]^{1/4} G_L^{-1/2} V_L^{-1/4} \quad (1)$$

(Hunt [H], cellular/ dendritic)

$$\lambda_1 = 4.3\left(\frac{\Gamma \Delta T D}{k_0}\right)^{1/4} G_L^{-1/2} V_L^{-1/4} \quad (2)$$

(Kurz and Fisher [KF], cellular /dendritic)

$$\lambda_1 = 4.09\, k_0^{-0.745}\left(\frac{\Gamma}{\Delta T}\right)^{0.41} D^{0.59} V_L^{-0.59} \quad (3)$$

(Hunt and Lu [HL], cellular)

*e-mail: amaurig@fem.unicamp.br

$$\lambda'_1 = 0.07798\, V'^{(a-0.75)}\, (V' - G')^{0.75}\, G'^{-0.6028} \quad (4)$$

(Hunt-Lu, dendritic)

where

$$a = -1.131 - 0.1555 \log_{10}(G') - 0.007589\, [\log_{10}(G')]^2 \quad (5)$$

$$\lambda'_1 = \frac{\lambda_1 \Delta T}{\Gamma k_0},\ G' = \frac{G_L \Gamma k_0}{\Delta T^2} \text{ and } V' = \frac{V_L \Gamma k_0}{D \Delta T} \quad (6)$$

where, λ_1 is the cellular and primary dendritic spacing, Γ is the Gibbs-Thomson coefficient, m_L is the liquidus line slope, k_0 the solute partition coefficient, C_0 is the alloy composition, D is the liquid solute diffusivity, ΔT is the difference between the liquidus (T_L) and solidus (T_S) equilibrium temperatures, V_L is the dendrite tip growth rate e G_L is the temperature gradient in front of the liquidus isotherm. Since the spacings proposed by Hunt and Lu (Eq. 3-6) refer to the radius rather than to the more commonly measured diameter and they are minimum spacings, the values need to be multiplied by 2 to 4 for comparison with measured spacings. Most of the unidirectional solidification studies existing in literature have been carried out with a view of characterizing cellular and primary spacings involving solidification in steady state heat flow. On the other hand, the analysis of these structures in the unsteady-state regime are very important, since it encompasses the majority of industrial solidification processes. The present article focuses on a theoretical/experimental investigation of cellular and primary dendritic spacings during the unsteady-state unidirectional solidification of Sn-Pb alloys.

2. Experimental Procedure

The casting assembly used in solidification experiments is shown in Fig. 1. The solidification apparatus was designed in such way the heat was extracted only through the water cooled bottom, promoting upward directional solidification. The use of such experimental configuration permits natural convection to be minimized, as well as solute convection due to buoyancy forces if the rejected solute has higher density than the alloy melt. A stainless steel mold was used having an internal diameter of 50 mm and height of 110 mm. The inner vertical surface was covered with a layer of insulating alumina to minimize radial heat losses, and a top cover made of an insulating material was used to reduce heat losses from the metal/air interface. The bottom part of the mold was closed with a thin (3 mm) disc of carbon steel. The alloys were melted *in situ* and the lateral electric heaters had their power controlled in order to permit a desired superheat to be achieved. To begin solidification, the electric heaters were disconnected and at the same time the water flow was initiated.

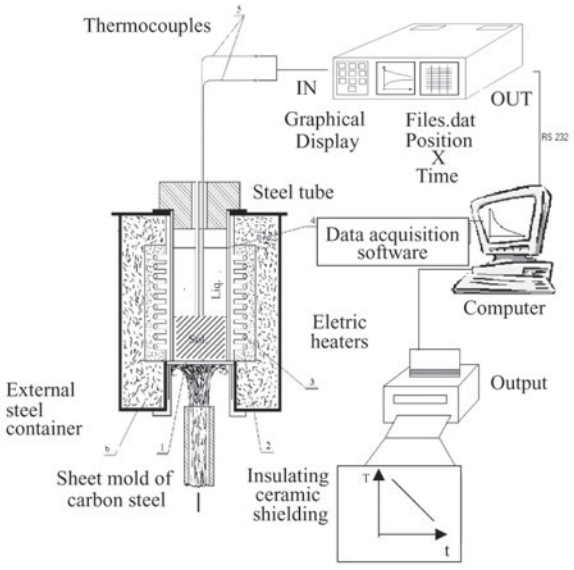

Figure 1. Experimental set-up used in unidirectional solidification experiments.

Experiments were carried out with Sn-Pb alloys (1.5; 2.5 and 5.0 wt% Pb) with superheats of 10% above the liquidus temperature. The thermophysical properties of these alloys are based on those reported in the literature[14]. The experiments were performed under a thermal contact condition at the metal/mold interface, corresponding to the heat extracting surface being polished.

Temperatures in the casting were monitored during solidification via the output of a bank of fine type K thermocouples, sheathed in 1.6 mm O.D. stainless steel protection tubes, and accurately positioned with regard to the heat-extracting surface. The thermocouples were calibrated at the melting temperature of tin exhibiting fluctuations of about 0.4 °C. Thermocouples readings were collected by a data acquisition system at a frequency of 0.5 s and stored on a computer.

Selected transverse sections of the directionally solidified specimens at 5, 10, 15, 20, 30, 40, 50, 60 and 70 mm from the metal/mold interface were electropolished and etched with an acid solution (50 ml glycerin, 35 ml acetic acid and 15 ml de HNO_3, 38 to 40 °C) for micrograph examination. Image processing systems Neophot 32 and Leica Quantimet 500 MC were used to measure cellular and dendrite spacings and their distribution range.

3. Results And Discussion

3.1. Solidification Thermal Parameters

The temperature files containing the experimentally monitored temperatures were used in a finite difference heat

flow program to determine the transient metal/mold heat transfer coefficient, h_i, as described in a previous article[14] , yield for all the three alloys examined:

$$h_i = 6000\ (t)^{-0.20}\ [W/m^2.K] \quad (7)$$

The experimental results of thermal analysis in metal have also been used to determine the displacement of liquidus isotherm, as well as tip growth rate as a function of time and position.

The tip growth rate can also be calculated by the analytical expression developed by Garcia[1,15], which was validated, in previous articles[14,16] against experimental values concerning the solidification of Al-Cu and Zn-Al alloys, respectively, and is given by:

$$V_L = \frac{2\alpha_{SL}\phi_2^{\,2}}{\left[\frac{2K_S\phi_2(T_S - T_0)}{n\sqrt{\pi}(T_L - T_0)\exp(\phi_1^{\,2})[M + \mathrm{erf}(\phi_1)]h_i}\right] + S_L} \quad (8)$$

where ϕ_1 and ϕ_2 are, respectively, solidification constants associated with the displacement of the solidus and liquidus isotherm, T_S is the non-equilibrium solidus temperature, T_0 is the environment temperature, T_L is the liquidus temperature, M is the ratio of heat diffusivities of solid and mold material, $(K_S c_S \rho_S / K_M c_M \rho_M)^{1/2}$ and n is the square root of the ratio of thermal diffusivities of solid metal and mushy zone, $(\alpha_S / \alpha_{SL})^{1/2}$, α_S is the solid thermal diffusivity ($K_S/c_S\rho_S$). The mushy zone thermal diffusivity, α_{SL} ($K_{SL}/c_{SL}\rho_{SL}$), is calculated by assuming the mushy properties as follows[15].

$$T > T_L \qquad K_L,\ \rho_L \text{ e } c_L; \quad (9)$$

$$T_S < T < T_L \quad K_{SL} = (K_S + K_L)/2 \quad (10)$$

$$\rho_{SL} = (\rho_S + \rho_L)/2 \quad (11)$$

$$c_{SL} = c_L + L(T_L - T_S) \quad (12)$$

$$T < T_{Sol} \quad K_S,\ r_S \text{ e } c_S \quad (13)$$

Equation 7 has been used by the analytical model, equation (8), in order to provide theoretical predictions for V_L.

Cosntants ϕ_1 and ϕ_2 can be determined by the simultaneous solution of the following equations:

$$\frac{(T_L - T_S)}{\mathrm{erf}(\phi_2) - \mathrm{erf}(n\phi_1)} = \frac{K_S \exp\left[(n^2 - 1)\phi_1^{\,2}\right]}{K_{SL}\, n\left[M + \mathrm{erf}(\phi_1)\right]}(T_S - T_0) \quad (14)$$

$$\frac{(T_L - T_S)}{\mathrm{erf}(\phi_2) - \mathrm{erf}(n\phi_1)} = \frac{K_L m \exp\left[(1 - m^2)\phi_2^{\,2}\right]}{K_{SL}\left[1 - \mathrm{erf}(m\phi_2)\right]}(T_P - T_L) \quad (15)$$

where m is the square root of ratio of thermal diffusivities of mushy zone and liquid, $(\alpha_{SL}/\alpha_L)^{1/2}$, α_S is the solid thermal diffusivity ($K_L/c_L\rho_L$) and T_p is the pouring temperature.

Figure 2 shows a comparison between the experimental results concerning solidification of the Sn-1.5; 2.5 and 5.0 wt% Pb compared to those calculated by the analytical approach, given by Eq. 8. Relatively good agreement can be observed.

Figures 3 and 4 show the experimental results of cellular and primary dendritic spacings as a function of tip growth rate and coling rate, respectively.

The cooling rate during solidification ($\dot{T}$) was calculated using the analytical mathematical expression developed by Garcia[1], given by:

$$\dot{T} = \frac{4m\phi_2(T_p - T_L)\alpha_L}{\sqrt{\pi}.[1 - \mathrm{erf}(m\phi_2)]\exp(m\phi_2)^2} V_L^{\,2} \quad (16)$$

where V_L is the experimental tip growth rate. The thermal gradient G_L can be determined by using values of $\dot{T}$ and V_L ($\dot{T} = G_L . V_L$).

In Fig. 2, it can be seen that the use of a water cooled mold imposes higher values of tip growth rates near the casting surface and a decreasing profile along the casting

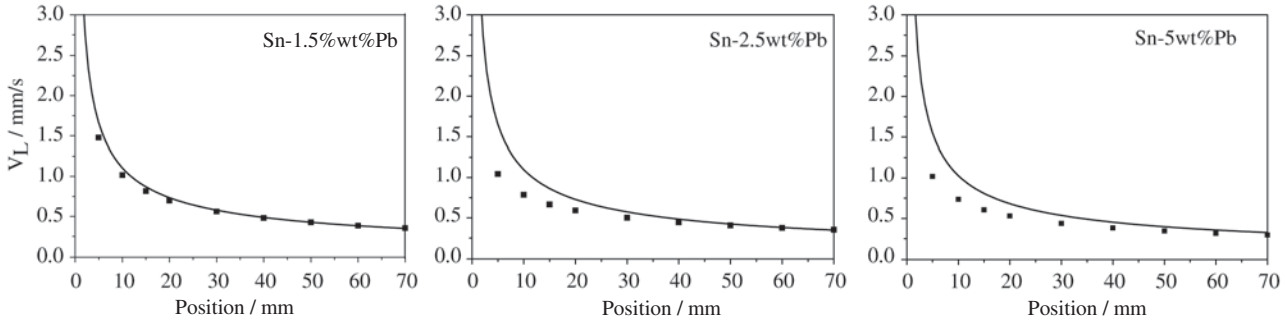

Figure 2. Comparison between experimental and analytical growth rate.

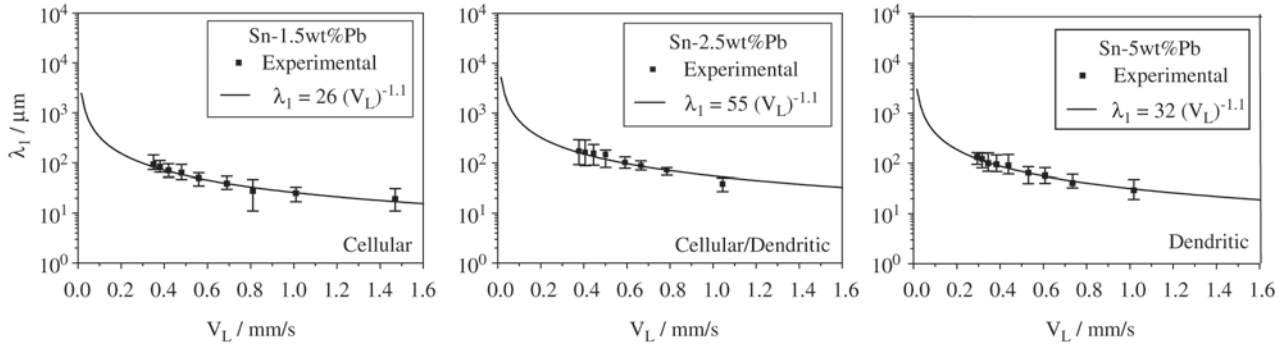

Figure 3. Cellular/Dendritic spacings as a function of tip growth rate.

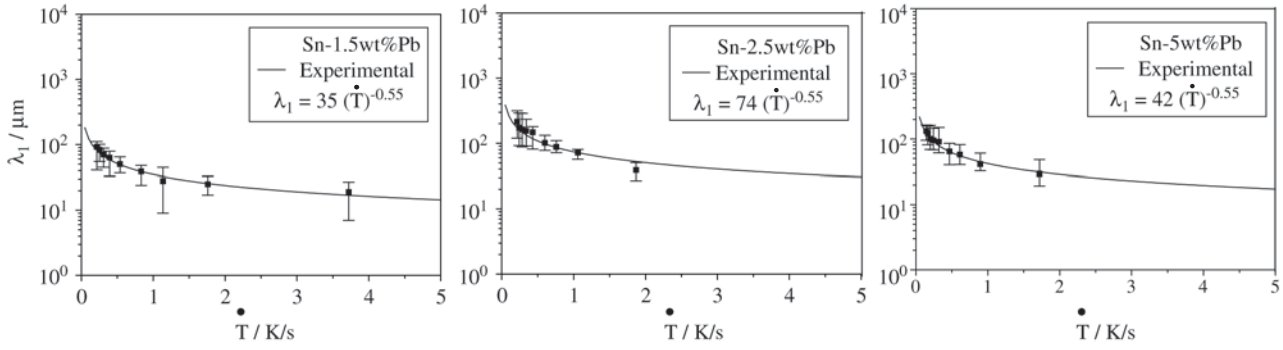

Figure 4. Cellular/Dendritic spacings as a function of cooling rate.

Table 1. Values used to calculate cooling rate and tip growth rate.

Material	m	n	ϕ_1	ϕ_2	α_L (m²/s)	α_{SL} (m²/s)	α_S (m²/s)
Sn-1.5%wtPb	0.496	3.0	0.403	1.893	1.82×10^{-5}	4.49×10^{-5}	4.12×10^{-5}
Sn-2.5%wtPb	0.491	3.0	0.405	1.906	1.81×10^{-5}	4.37×10^{-5}	4.09×10^{-5}
Sn-5%wtPb	0.477	3.15	0.409	1.981	1.81×10^{-5}	4.07×10^{-5}	4.04×10^{-5}

due to the increasing thermal resistance of the solidified shell with distance from the cooled surface. This influence translates to the observed experimental values of cellular and dendritic spacings as shown in Figs. 3 and 4, where average spacings along with the standard variation are presented. Values of α_S, α_{SL}, α_L, m, ϕ_1 and ϕ_2 for the alloys and conditions adopted for experimentation are presented in Table 1.

Figure 5 presents a comparison between experimental values of cellular and primary spacings with theoretical predictions furnished by the Hunt-Lu model. It can be seen that for cellular growth, the upper limit of the Hunt-Lu model best matches the experimental observations. For dendritic growth, an opposite situation is observed with the lower limit of the Hunt-Lu model best fitting the experimental results.

Figure 6 shows comparisons between experimental cellular and dendritic spacings and predictions furnished by Hunt and Kurz-Fisher models, which consider solidification in steady-state heat flow conditions. It can be seen that despite the experimental values were obtained in unsteady-state solidification, the experimental points appear to agree reasonably well with the results furnished by Hunt's model, in any case experimentally examined. The results calculated by using Kurz and Fisher model are far from those observed experimentally. A similar observation has been reported in a recent article dealing with the steady-sate solidification of lead alloys[12].

3.2 Cellular/Dendritic Transition

Typical microstructures observed along the cross and longitudinal sections of Sn 1.5wt%Pb, Sn 2.5wt%Pb and Sn 5wt%Pb castings are shown respectively in Figs. 7, 8 and 9. The microstructures observed from bottom to top

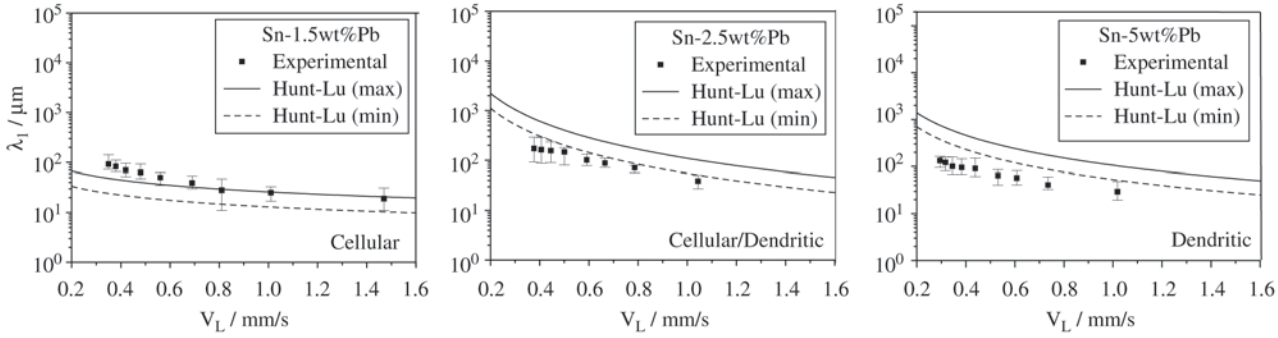

Figure 5. Comparison between theoretical and experimental values of cellular/dendritic spacings.

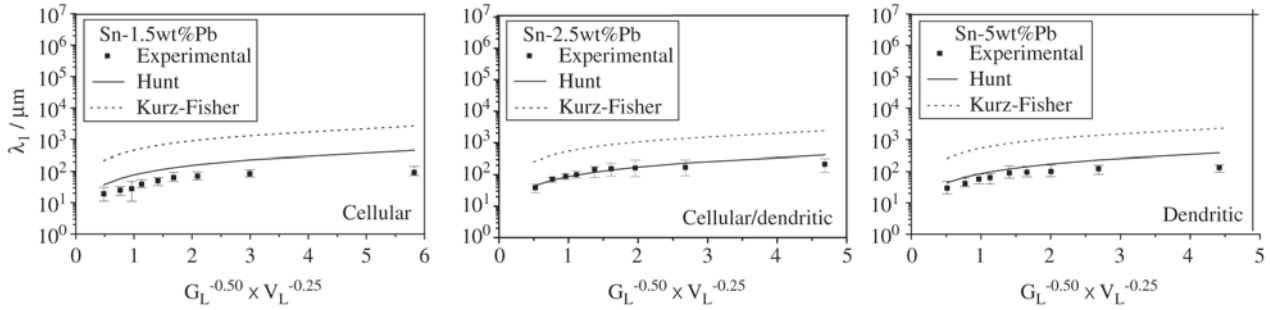

Figure 6. Comparison between theoretical and experimental values of cellular/dendritic spacings

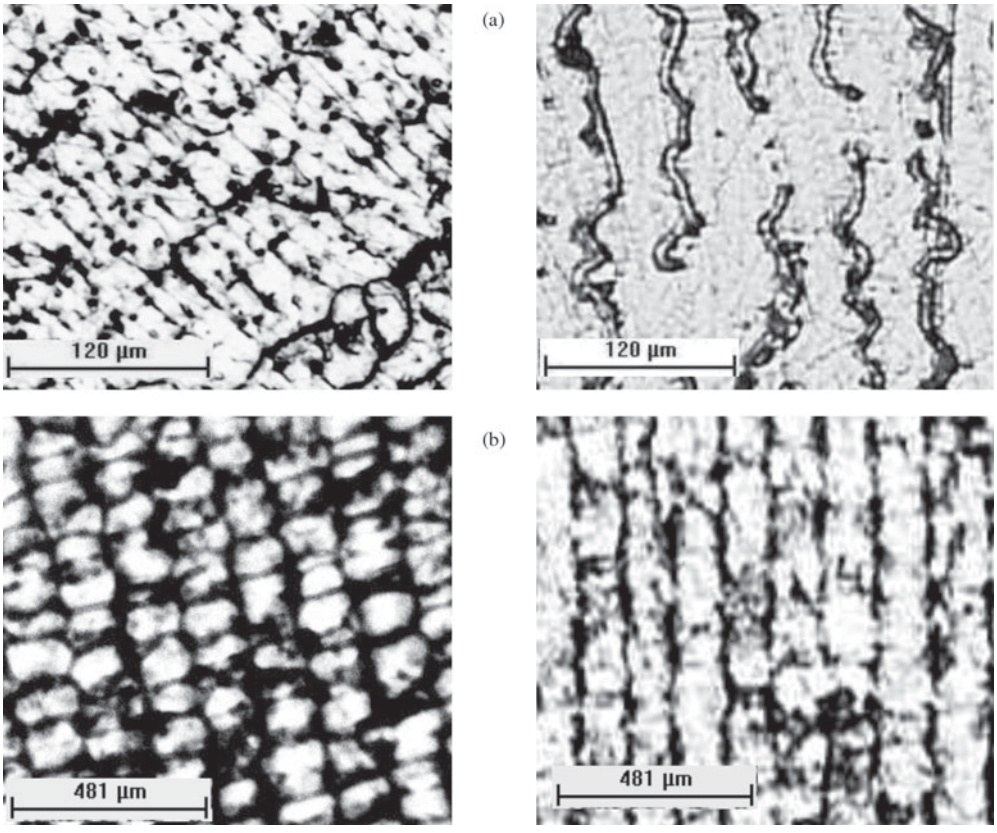

Figure 7. Resulting microstructure for Sn-2.5wt%Pb alloy: a) celullar/dendritic P = 5 mm, λ_1= 39 mm, V_L= 1.04 mm/s, $\dot{T}$= 1.8 K/s; b) cellular P = 50 mm, λ_1=163 mm, V_L= 0.4 mm/s, $\dot{T}$= 0.28 K/s.

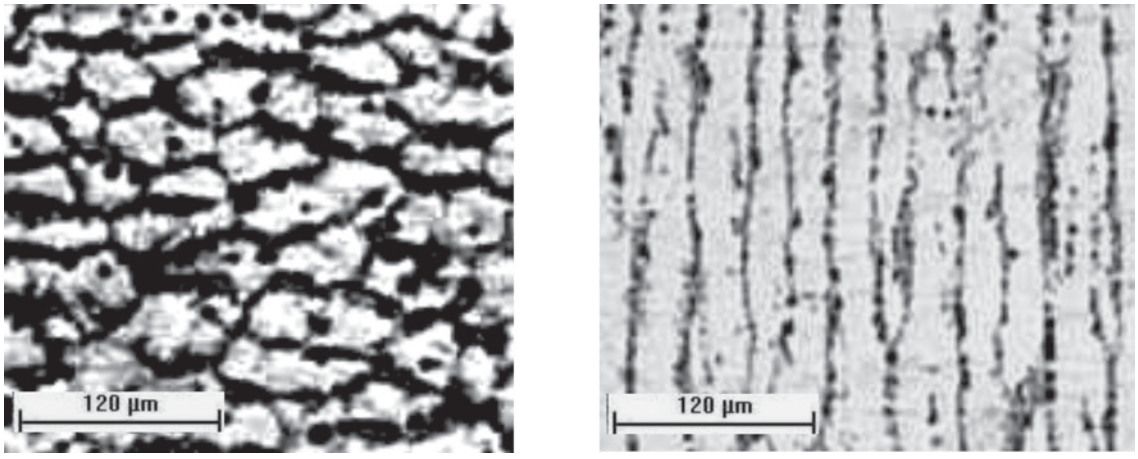

Figure 8. Cellular microstructure for Sn-1.5wt%Pb alloy (P = 10 mm, λ_1= 25 mm, V_L= 1.01 mm/s and $\dot{T}$ = 1.75 K/s) .

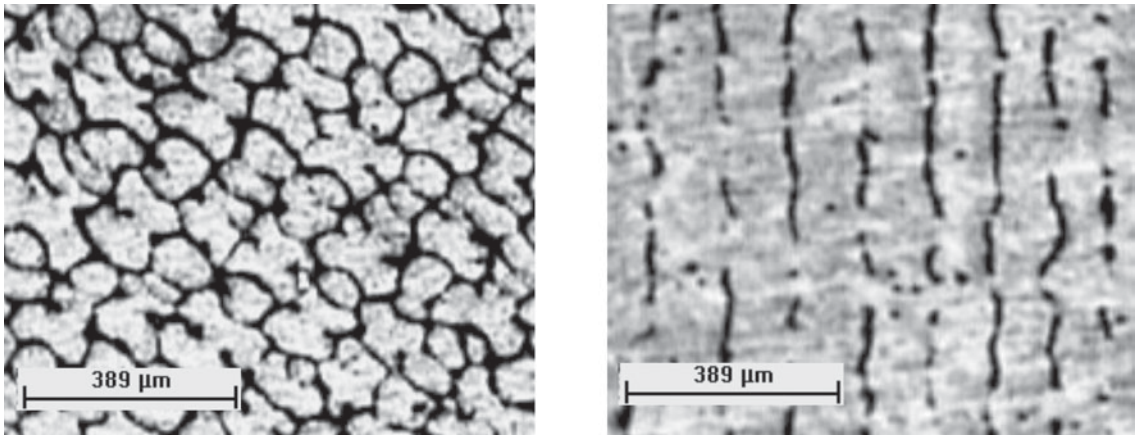

Figure 9. Dendritic microstructure for Sn-5wt%Pb alloy (P = 40 mm, λ_1= 95 mm, V_L= 0.38 mm/s and $\dot{T}$ = 0.24 K/s).

along the Sn 1.5wt%Pb ingot were always cellular, while a dendritic pattern was observed along the Sn 5wt%Pb casting which included well defined side perturbations conducive to secondary arms. The cellular/dendritic transition occurred during the unidirectional growth of the Sn 2.5wt%Pb ingot, with lateral perturbations beginning to appear under a cooling rate of about 0.28 K/s and being clearly defined when a cooling rate of about 1.86 K/s was reached.

4. Conclusions

Under unsteady-state solidification conditions the cellular/primary dendritic spacings were observed to decrease when tip growth rate and cooling rate are increased.

The upper limit of the Hunt-Lu cellular growth model closely matched the experimental spacings. The lower limit calculated with the Hunt-Lu dendritic model best generated the experimental results. On the other hand, the experimental points appear to agree reasonably well with the results furnished by Hunt's model, in any case experimentally examined, in spite of the assumption of steady state heat flow conditions considered in the development of this model. The results calculated by using Kurz and Fisher model (steady-state) are far from those observed experimentally.

The cellular/dendritic transition was observed to occur for the Sn 2.5wt%Pb alloy over a range of cooling rates from 0.28 K/s to 1.8 K/s. For the Sn 1.5wt%Pb and the Sn 5wt%Pb castings, the observed microstructures were totally cellular and dendritic, respectively.

Acknowledgements

The authors acknowledge financial support provided by CNPq (The Brazilian Research Council), FAPESP (The

Scientific Research Foundation of the State of São Paulo, Brazil), UNICAMP and CEFET – Pará.

References

1. Garcia, A. Solidification: Fundamentals and Applications, Ed. Unicamp, São Paulo, Brazil, p. 201-242, 2001.
2. Hunt, J.D. International Conference on Solidification and Casting of Metals, London, Metals Society, p.3-9, 1979.
3. Kurz, W.; Fisher, D.J, Fundamentals of Solidification, *Trans Tech Publications*, Switzerland, p. 85-87, 1992.
4. Hunt, J.D.; Lu, S.Z. *Metallurgical and Materials Transactions A*, v. 27A, p. 611-623, 1996**.**
5. Trivedi, R. *Metallurgical and Materials Transactions A*, v. 15A, n. 6, p. 977-982, 1984.
6. Trivedi, R.; Kurz, W., *International Materials Review*, v. 39, n. 2, p. 49-74, 1994.
7. Koseki, T.; Flemings, M.C., *Iron Steel Institute Japan Int.*, v. 35, n. 6, p. 611-617, 1995
8. Kirkaldy, J.S.; Bouchard, D., *Metallurgical and Materials Transactions B*, v. 28B, p.651-663, 1997.
9. Feng, J.; Huang, W.D.; Lin, X.; Pan, Q.Y.; Li, T.; Zhou Y.H. *Journal of Crystal Growth*, v.197, p.393-395, 1999.
10. Feng, J.; Huang, W.D.; Lin, X.; Pan, Q.Y.; Li, T.; Zhou Y.H. *Acta Materialia*, v. 47, n. 11, p.3271-3280, 1999.
11. Yu, L.; Ding, G.L.; Reye, J.; Ojha, S.N.; Tewari, S.N. *Metallurgical and Materials Transaction A*, v. 30A, p.2463-2471, 1999.
12. Cardili, E.; Gündüz, M. *Journal of Materials Science*, v. 35, p. 3837-3848, 2000
13. Santos, C.A.; Quaresma, J.M.V.; Garcia, A. *Journal of Alloys and Compounds*, v. 319, p.174-186, 2001.
14. Quaresma, J.M.V.; Santos, C.A.; Garcia, A. *Metallurgical and Materials Transactions*, v. 31A, p.3167-3178, 2000.
15. Garcia, A; Prates, M. *Metallurgical Transactions*, v. 9B, p. 449-457, 1978.
16. Osório, W.R.; Garcia A. *Materials Science and Enginnering*, A325, p. 103-111, 2002.